Int. J. Heat Mass Transfer. Vol. 16, pp. 2241–2260. Pergamon Press 1973. Printed in Great Britain

THE SECOND-ORDER BOUNDARY LAYER ALONG A CIRCULAR CYLINDER IN SUPERSONIC FLOW

K. GERSTEN
Institut für Thermo- und Fluiddynamik, Ruhr-Universität Bochum, FRG

and

J. F. GROSS
Department of Chemical Engineering, University of Arizona, Tucson, Arizona 85721, U.S.A.
and
Rand Corporation, Santa Monica, California 90406, U.S.A.

(*Received* 27 *December* 1972)

Abstract—The second-order laminar boundary layer along a circular cylinder in supersonic flow with and without surface mass transfer is studied using the method of matched asymptotic expansions. Specifically, the analysis obtains the second-order terms for the pressure, the shear stress, and the heat transfer at the wall due to transverse surface curvature and displacement. For the flow near the leading edge of the cylinder numerical results are presented.

There are three second-order effects, namely due to transverse curvature, due to displacement, and due to interaction of curvature and displacement.

For the solid wall all three second-order effects increase the shear stress and this result increases with increasing wall temperature. In the case of heat transfer, the displacement effect vanishes, the interaction effect is always positive (increasing the heat transfer), and the transverse curvature effect is positive for small wall temperatures and negative for large wall temperatures.

The effect of mass flow at the wall is generally in the expected direction; i.e. the injection of mass thickens the boundary layer and increases second-order effects whereas wall suction, by extracting mass from the boundary layer, reduces the importance of displacement and transverse curvature. An exception to the general rule stated above occurs at high wall temperatures.

NOMENCLATURE

a, speed of sound;
A_0, constant in equation (33);
B, $\sqrt{(M^2 - 1)}$;
B_n, $n = 0, 1, 2, \ldots$ constants in equation (34);
c_f, local skin friction coefficient defined by equation (15):
c_M, mass transfer parameter defined by equation (12);
c_p, specific heat capacity of constant pressure;
c_{pw}, wall pressure coefficient defined by equation (14);
C, Chapman–Rubesin parameter defined by equation (1);
C_τ, coefficient representing the transverse curvature effect on wall shear stress defined by equation (90);
C_q, coefficient representing the transverse curvature effect on wall heat flux defined by equation (91);
D_τ, coefficient representing the displacement effect on wall shear stress defined by equation (90);
E, $(\gamma - 1) M^2/2$, Eckert number;
$f(\eta)$, nondimensional stream function defined by equation (39);
$f_0(\eta), f_1(\eta)$, nondimensional stream functions defined by equation (68);

$F_n(\eta)$, $n = 0, 1, \ldots$, functions defined by equation (57);
$g(\eta)$, nondimensional temperature function defined by equation (43);
$g_0(\eta)$, $g_1(\eta)$, nondimensional temperature functions defined by equation (69);
$G_n(\eta)$, $n = 0, 1, \ldots$, functions defined by equation (57);
$I_1(\lambda)$, modified Bessel function;
I_τ, coefficient representing the interaction effect on wall shear stress defined by equation (90);
I_q, coefficient representing the interaction effect on wall heat flux defined by equation (91);
k, thermal conductivity;
$K_1(\lambda)$, modified Bessel function;
M, Mach number;
p, nondimensional static pressure defined by equation (2);
q_w, local heat flux at the wall;
r, $1 + y$, nondimensional radial coordinate;
r_0, radius of the cylinder;
R, Reynolds number defined by equation (9);
St, Stanton number defined by equation (16);
T, nondimensional temperature based on T_∞;
T_w, wall temperature;
T_∞, free-stream temperature;
u, nondimensional velocity component in x-direction of the inner solution;
U, nondimensional velocity component in x-direction of the outer solution;
U_∞, free-stream velocity;
v, nondimensional velocity component in y-direction of the inner solution;
V, nondimensional velocity component in y-direction of the outer solution;
$W(z)$, function defined by equation (31);
x, nondimensional axial coordinate;
y, nondimensional coordinate perpendicular to the wall;
$\bar{y}$, y/ε stretched coordinate;
z, variable used in equations (31) and (32);
γ, ratio of heat capacities;
ε, perturbation parameter defined by equation (17);
η, nondimensional inner variable defined by equation (36);
$\bar{\eta}$, variable defined by equation (38);
$\theta(x, \eta)$, second order temperature function defined by equation (43);
λ, variable in equation (31);
μ, nondimensional viscosity, based on free-stream viscosity;
ρ, nondimensional density based on free-stream density;
σ, Prandtl number;
τ_w, wall shear stress;
ϕ, potential function defined by equation (24);
$\psi(x, y)$ second order stream function defined by equation (39);
γ, viscous interaction parameter defined by equation (78);
ω, vorticity in the outer flow defined by equation (20).

Subscripts

∞, undisturbed free stream;
w, wall;
w_a, adiabatic wall;
1, first order;
10, first order for $M = 0$ and $T_w = 0$;
2, second order.

Superscript

*, dimensional quantities.

1. INTRODUCTION

It is well known that the classical Prandtl boundary-layer theory is valid only when two basic requirements are fulfilled: (1) the boundary-layer thickness must be small compared with a characteristic curvature dimension of the body surface and (2) the rate of growth of the boundary layer must be small. In this way, the curvature of the flow in the boundary layer as well as the displacement effect of the boundary layer on the inviscid free-stream flow can be completely neglected.

In many practical situations, however, these basic requirements are not fulfilled and, therefore, the use of the Prandtl boundary-layer theory is not justified. Examples of flows in which relatively thick boundary layers occur include high supersonic or hypersonic flows where viscous heating reduces the density and hence increases the thickness of the boundary layer. Ablation and transpiration cooling also thicken the boundary layer by the introduction of additional mass. Thick boundary layers can also occur at the rear of long slender bodies; the boundary layer has continued to grow by entrainment from the free stream so that its thickness can no longer be neglected.

A higher-order theory is necessary in order to study the effects of body curvature and displacement on the behaviour of the boundary layer. Van Dyke [1–4] has given careful and extensive treatments of this theory to obtain solutions for the Navier–Stokes equations at high Reynolds numbers using the method of matched asymptotic expansions. The classical boundary-layer theory represents the first approximation to the solution. The second approximation, usually referred to as second-order boundary-layer theory provides a systematic framework to study the effects of body curvature and displacement. Other second-order effects can also arise from external gradients of entropy and enthalpy (vorticity) or from velocity slip and a temperature jump at the wall; these will, however, not be considered here.

Few studies have been made in which the second-order effects resulting from curvature and displacement have been completely and properly treated. The reason is that determination of the second-order effects is only possible at the present time if the boundary layer does not separate. Complete solutions of the second-order boundary layer exist only for the parabola (Van Dyke [5]) and the Rankine half body (Devan [6]). In both cases, the longitudinal curvature effect and the displacement effect are treated. The extension of these solutions to include mass flow at the wall is given by Gersten and Gross [7] and Gersten *et al.* [8]. In the case of wall injection particularly, the second-order effects which result from boundary layer thickening can be greatly enhanced.

A body which has only transverse curvature is the circular cylinder whose axis is parallel to the free-stream flow. For this body, the effect of curvature alone has been investigated for the case of incompressible flow by Seban and Bond [9], Kelly [10], Cooke [11], Glauert and Lighthill [12], Eshgy and Hornbeck [13], Wanous and Sparrow [14], Jaffe and Okamura [15] and Cebeci *et al.* [16]. These solutions are not complete, however, because the displacement effect is missing and only incompressible flow is considered.

Consider the supersonic flow along the outer surface of hollow circular cylinder whose axis is parallel to the free stream. The effects of transverse curvature and boundary-layer displacement as well as those of mass flow at the wall will be studied. It is assumed that the flow inside the cylinder cannot affect the flow on the outer surface.

The purpose of the present work is to determine the second-order effects resulting from transverse curvature and displacement on the induced wall pressure, wall shear stress, and wall heat transfer. Further, it will be shown how mass flow at the wall (injection and suction) influence these second-order effects.

2. BASIC EQUATIONS

We consider the supersonic flow of velocity

U_∞ along the surface of a cylinder with radius r_0 and with its axis parallel to the flow direction (see Fig. 1). The coordinates in the axial and

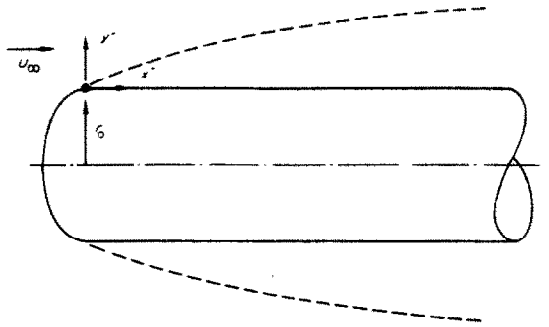

FIG. 1. Coordinate system for circular cylinder in axial flow.

radial directions are x^* and y^*, respectively [( )* indicates dimensional variable]. An ideal gas with constant specific heat, c_p, is assumed. The Prandtl number $\sigma = c_p\mu^*/k^*$ is kept constant so that the viscosity, μ^*, and the thermal conductivity, k^*, have the same dependence on the temperature, T^*. The following assumption for the viscosity variation is made:

$$\rho^*\mu^* = \rho_w\mu_w = C\rho_\infty\mu_\infty \tag{1}$$

when the indices w and ∞ refer to the wall and free-stream, respectively. In equation (1), C is the well-known Chapman–Rubesin coefficient.

Rotational symmetry reduces the velocity to two components: u^* in the x^* direction and v^* in the y^* direction. The variables are made nondimensional as follows:

$$x = \frac{x^*}{r_0} \qquad y = \frac{y^*}{r_0}$$

$$u = \frac{u^*}{U_\infty} \qquad v = \frac{v^*}{U_\infty} \tag{2}$$

$$p = \frac{p^* - p_\infty}{\rho_\infty U_\infty^2}, \quad \rho = \frac{\rho^*}{\rho_\infty}, \quad T = \frac{T^*}{T_\infty}, \quad \mu = \frac{\mu^*}{\mu_\infty}.$$

The five dependent variables are the velocity components $u(x, y)$ and $v(x, y)$, the static pressure $p(x, y)$, the density $\rho(x, y)$, and the temperature $T(x, y)$. By $r = 1 + y$ the flow equations for this system are given by:

$$\frac{\partial}{\partial x}(\rho r u) + \frac{\partial}{\partial y}(\rho r v) = 0 \tag{3}$$

$$\rho u\frac{\partial u}{\partial x} + \rho v\frac{\partial u}{\partial y} = -\frac{\partial p}{\partial x} + \frac{1}{R}\left\{2\frac{\partial}{\partial x}\left(\mu\frac{\partial u}{\partial x}\right) + \frac{1}{r}\frac{\partial}{\partial y}\left(\mu r\frac{\partial u}{\partial y}\right) + \frac{1}{r}\frac{\partial}{\partial y}\left(\mu r\frac{\partial v}{\partial x}\right) - \frac{2}{3}\frac{\partial}{\partial x}\left[\mu\left(\frac{\partial u}{\partial x} + \frac{\partial v}{\partial y} + \frac{v}{r}\right)\right]\right\} \tag{4}$$

$$\rho u\frac{\partial v}{\partial x} + \rho v\frac{\partial v}{\partial y} = -\frac{\partial p}{\partial y} + \frac{1}{R}\left\{\frac{2}{r}\frac{\partial}{\partial y}\left(\mu r\frac{\partial v}{\partial y}\right) - \frac{2\mu}{r^2}v + \frac{\partial}{\partial x}\left(\mu\frac{\partial u}{\partial y}\right) + \frac{\partial}{\partial x}\left(\mu\frac{\partial v}{\partial x}\right) - \frac{2}{3}\frac{\partial v}{\partial y}\left[\mu\left(\frac{\partial u}{\partial x} + \frac{\partial v}{\partial y} + \frac{v}{r}\right)\right]\right\} \tag{5}$$

$$\rho u\frac{\partial T}{\partial x} + \rho v\frac{\partial T}{\partial y} = 2E\left(u\frac{\partial p}{\partial x} + v\frac{\partial p}{\partial y}\right) + \frac{1}{\sigma R}\left[\frac{\partial}{\partial x}\left(\mu\frac{\partial T}{\partial x}\right) + \frac{1}{r}\frac{\partial}{\partial y}\left(\mu r\frac{\partial T}{\partial y}\right)\right] + \frac{2E}{R}\mu\Phi \tag{6}$$

where Φ is the dimensionless dissipation function given by

$$\Phi = 2\left[\left(\frac{\partial u}{\partial x}\right)^2 + \left(\frac{\partial v}{\partial y}\right)^2 + \left(\frac{v}{r}\right)^2\right] + \left(\frac{\partial v}{\partial x} + \frac{\partial u}{\partial y}\right)^2 - \frac{2}{3}\left(\frac{\partial u}{\partial x} + \frac{\partial v}{\partial y} + \frac{v}{r}\right)^2. \tag{7}$$

The equation of state is

$$p = \frac{\gamma - 1}{\gamma}\frac{1}{2E}(\rho T - 1) = \frac{1}{\gamma M^2}(\rho T - 1). \tag{8}$$

The above equations contain the following dimensionless parameters:

Reynolds number:

$$R = \frac{\rho_\infty U_\infty r_0}{\mu_\infty}$$

Eckert number:

$$E = \frac{U_\infty^2}{2c_p T_\infty} = \frac{\gamma - 1}{2} M^2 \quad (9)$$

Mach number:

$$M = \frac{U_\infty}{a_\infty}.$$

Here, the dimensional sound velocity in the free-stream is designated by a_∞. The speed of sound, a^*, is given by:

$$a^{*2} = \left(\frac{\partial p^*}{\partial \rho^*}\right)_s = \gamma \frac{p^*}{\rho^*} = c_p(\gamma - 1)\, T^*. \quad (10)$$

In the free-stream, this becomes:

$$a_\infty^2 = \gamma \frac{p_\infty}{\rho_\infty} = c_p(\gamma - 1)\, T_\infty. \quad (11)$$

For simplicity we assume that the normal wall velocity $v_w \sim 1/\sqrt{x}$. Therefore, the boundary conditions for this system are:

At the wall:

$$y = 0 \qquad u = 0$$

$$\rho v = \frac{\rho_w v_w}{\rho_\infty U_\infty} = -\frac{\varepsilon\sqrt{C}}{2\sqrt{x}} C_M \quad (12)$$

$$T = \frac{T_w}{T_\infty} = \text{constant}$$

where C_M is constant and designated as the wall mass transfer parameter. For the case of mass injection, $C_M < 0$. and $C_M > 0$ for suction at the wall. The parameter ε is given by equation (7).

In the free-stream:

$$\begin{aligned} x < 0 \qquad & u = 1 \\ & v = 0 \\ & p = 0 \\ & \rho = 1 \\ & T = 1. \end{aligned} \quad (13)$$

The functions $p_w(x)$ and $\rho_w(x)$ are unknowns and will be found as part of the solutions to the equations.

The dimensionless parameters γ, σ, C, R, E (or M), T_w/T_∞, and C_M are prescribed and it is required to find the unknown dependent variables $u(x, y)$, $v(x, y)$, $p(x, y)$, $\rho(x, y)$, and $T(x, y)$. In particular, we wish to determine the distribution of pressure and density at the wall:

$$c_{pw}(x) = \frac{p_w(x) - p_\infty}{\rho_\infty U_\infty^2} = p(x, 0),$$

$$\frac{\rho_w(x)}{\rho_\infty} = \rho(x, 0). \quad (14)$$

The wall shear stress:

$$c_f(x) = \frac{\tau_w(x)}{\rho_\infty U_\infty^2} = \frac{C}{R} \frac{\rho_\infty}{\rho_w(x)} \left(\frac{\partial u}{\partial y}\right)_{y=0} \quad (15)$$

and the heat transfer at the wall (Stanton-number):

$$St(x) = \frac{q_w(x)}{c_p \rho_\infty U_\infty T_\infty} = -\frac{C}{\sigma R} \frac{\rho_\infty}{\rho_w(x)} \left(\frac{\partial T}{\partial y}\right)_{y=0} \quad (16)$$

We are concerned with solutions of the equations at large values of the Reynolds number, i.e. for $R \to \infty$. The solutions will be obtained using the method of matched asymptotic expansions where the perturbation parameter ε is given by:

$$\varepsilon = \frac{1}{\sqrt{R}} = \sqrt{\left(\frac{\mu_\infty}{r_0 U_\infty \rho_\infty}\right)}. \quad (17)$$

The solutions will be obtained by appropriately matching inner and outer expansions which satisfy the inner and outer boundary conditions, respectively. The inner solution will then yield the required wall functions.

3. OUTER EXPANSION

The following expansions are assumed for the outer flow:

$$u = U_1(x, y) + \varepsilon U_2(x, y) + \dots$$
$$v = V_1(x, y) + \varepsilon V_2(x, y) + \dots$$
$$p = P_1(x, y) + \varepsilon P_2(x, y) + \dots \quad (18)$$
$$\rho = R_1(x, y) + \varepsilon R_2(x, y) + \dots$$
$$T = T_1(x, y) + \varepsilon T_2(x, y) + \dots$$

Substituting these expansions in the flow equations and matching with the undisturbed free-stream conditions yields the first-order terms directly:

$$U_1 = 1, V_1 = 0, P_1 = 0, R_1 = 1, T_1 = 1. \quad (19)$$

The second-order terms are obtained by substituting the above expansions into equations (3)–(8) and collecting terms according to powers of ε. This gives a set of five equations for second order terms: $U_2(x, y)$, $V_2(x, y)$, $P_2(x, y)$, $R_2(x, y)$ and $T_2(x, y)$.

Elimination of P_2 in the second-order momentum equation yields the vorticity in the outer flow:

$$\frac{\partial V_2}{\partial x} - \frac{\partial U_2}{\partial y} = \omega(y) \quad (20)$$

where $\omega(y)$ is the constant of integration which remains to be obtained from the boundary conditions. Since we have assumed no vorticity in the undisturbed free-stream, any vorticity which occurs must result from the presence of curved shock waves. It will be shown that the second-order terms, which represent a correction to the undisturbed free-stream, are solutions to the linearized potential flow equation. Therefore, within the context of second-order theory, no shock waves and hence no vorticity in the outer expansion can occur. It is always true that:

$$\frac{\partial V_2}{\partial x} - \frac{\partial U_2}{\partial y} = 0. \quad (21)$$

Therefore, the entropy in the entire outer field is also constant. Equation (10) for the speed of sound can be written:

$$a^{*2} = \left(\frac{\partial p^*}{\partial \rho^*}\right)_s = U_\infty^2 \frac{\partial P_2}{\partial R_2} = a_\infty^2(1 + \varepsilon T_2). \quad (22)$$

The difference between a^2 and a_∞^2 is small, of $0(\varepsilon)$, and can be neglected. It follows then that the continuity equation for the outer flow becomes:

$$(1 - M^2)\frac{\partial U_2}{\partial x} + \frac{V_2}{1 + y} + \frac{\partial V_2}{\partial y} = 0. \quad (23)$$

Equation (21) for the vorticity can be satisfied by a potential function ϕ:

$$U_2 = \frac{\partial \phi}{\partial x} \qquad V_2 = \frac{\partial \phi}{\partial y}. \quad (24)$$

The substitution of equation (24) into equation (23) yields the well-known potential equation for axisymmetric flow:

$$(1 - M^2)\phi_{xx} + \phi_{yy} + \frac{1}{1 + y}\phi_y = 0. \quad (25)$$

The third term in equation (25) represents the difference between two-dimensional and axisymmetric flow.

The unknown potential function must satisfy the following boundary condition

$$\phi_y|_{y=0} = V_2(x, 0) \quad (26)$$

where $V_2(x, 0)$ is obtained by matching the inner and outer expansions and can be considered as known. Having obtained $\phi(x, y)$, the five unknown functions are immediately given by

$$U_2(x, y) = \phi_x$$
$$V_2(x, y) = \phi_y$$
$$P_2(x, y) = -U_2(x, y) = -\phi_x \quad (27)$$
$$R_2(x, y) = \frac{2\gamma E}{\gamma - 1} P_2(x, y) - T_2(x, y) = -\frac{2E}{\gamma - 1}\phi_x$$
$$T_2(x, y) = 2EP_2(x, y) = -2E\phi_x.$$

For the matching process, it is of particular interest to obtain the velocity components in the x-direction at the wall; i.e.

$$U_2(x, 0) = \phi_x(x, 0). \quad (28)$$

Several methods are available to solve the potential equation, equation (25), with the boundary

condition, equation (26). If one does not require the solution $\phi(x, y)$ specifically, but only the relationship between $V_2(x, 0)$ and $U_2(x, 0)$, then the operator method can be used. Ward [17] has shown that the relationship between $V_2(x, 0)$ and $U_2(x, 0)$ is given by

$$U_2(x,0) = -\frac{1}{B}\left\{V_2(x,0) - \frac{1}{B}\int_0^x W\left(\frac{x-\xi}{B}\right) V_2(\xi,0)\,d\xi\right\} \quad (29)$$

with

$$B = \sqrt{(M^2 - 1)}. \quad (30)$$

The function $W(z)$ is given by:

$$W(z) = \int_0^\infty \frac{e^{-\lambda z}}{K_1^2(\lambda) + \pi^2 I_1^2(\lambda)} \frac{d\lambda}{\lambda} \quad z \geqslant 0 \quad (31)$$

where $K_1(\lambda)$ and $I_1(\lambda)$ are modified Bessel functions. The function $W(z)$ is given by Ward [17]. The expansion for $W(z)$, when z is small, is given by

$$W(z) = \tfrac{1}{2} - \tfrac{3}{8}z + \tfrac{3}{16}z^2 - \ldots \qquad 0 \leqslant z < 2. \quad (32)$$

Solutions near the leading edge, i.e. for small x, will be examined more closely. The function $V_2(x, 0)$ can be written in the form

$$V_2(x,0) = \frac{A_0}{x}. \quad (33)$$

If we use the expansion for $W(z)$ for small z [equation (32)], then equation (29) yields

$$U_2(x,0) = \frac{1}{\sqrt{x}} \sum_0^N B_n x^n. \quad (34)$$

The initial coefficients are then given by

$$B_0 = -\frac{A_0}{B}, \qquad B_1 = \frac{A_0}{B^2}, \qquad B_2 = -\frac{1}{2}\frac{A_0}{B^3}. \quad (35)$$

4. INNER EXPANSION

For the inner expansion, a new variable, η, is defined as follows:

$$\eta = \frac{1}{\varepsilon}\frac{1}{2\sqrt{(Cx)}}\int_0^y \rho(1+y)\,dy. \quad (36)$$

The effect of ρ, the density, can be accounted for by the Dorodnitsyn–Howarth transformation which transforms the compressible flow problem to an incompressible one. Equation (36) can be written:

$$y = \varepsilon 2\sqrt{(Cx)}\int_0^\eta \frac{d\eta}{\rho} + 0(\varepsilon^2). \quad (37)$$

It can be seen that η [see equation (36)] and $\bar{\eta}$ defined by:

$$\bar{\eta} = \frac{1}{2\sqrt{(Cx)}}\int_0^y \rho\,dy \quad (38)$$

differ only by $0(\varepsilon)$. For an incompressible flow, $\bar{\eta}$ reduces to the well-known similarity variable for first-order boundary-layer theory (Dewey and Gross [18]). In that case, the function y/ε would have sufficed for the inner variable. The generalization of η given in equation (36) has been chosen to simplify the equations.

The five unknowns are functions of x and η only and the following analytical asymptotic expansions are assumed:

$$u = \tfrac{1}{2}f' + \varepsilon\frac{\sqrt{C}}{2}\psi_\eta + 0(\varepsilon^2) \quad (39)$$

$$v = -\frac{1}{4}\varepsilon\sqrt{\left(\frac{C}{x}\right)}(fg' - gf') + 0(\varepsilon^2) \quad (40)$$

$$p = \varepsilon\sqrt{(C)}p_2 + 0(\varepsilon^2) \quad (41)$$

$$\frac{1}{\rho} = T(1 + \gamma M^2 p)^{-1} = \tfrac{1}{2}g' + \varepsilon(\sqrt{C})(\tfrac{1}{2}\theta_\eta - \tfrac{1}{2}\gamma M^2 p_2 g') + 0(\varepsilon^2) \quad (42)$$

$$T = \tfrac{1}{2}g' + \varepsilon\frac{\sqrt{C}}{2}\theta_\eta + 0(\varepsilon^2). \quad (43)$$

Here the indices x and η denote partial differentiation and primes indicate d( )/dη. The expansions for u and v have been selected so that continuity is satisfied. The value for v at the wall is given by

$$(\rho v)_w = \frac{\rho_w v_w}{\rho_\infty U_\infty} = -\frac{\varepsilon}{2}\sqrt{\left(\frac{C}{x}\right)} f(0) - \varepsilon^2 C\left(\sqrt{(x)}\psi_x + \frac{1}{2\sqrt{x}}\psi\right) + 0(\varepsilon^3). \quad (44)$$

Inspection of the y-momentum equation, equation (5), shows that for the pressure p no absolute term can be obtained and that the term proportional of ε is independent of η, i.e. $p_2 = p_2(x)$.

Substitution of equations (39)–(43) into the x-momentum equation, equation (4), and the energy equation, equation (6), yields the following differential equations for the unknowns $f(\eta)$, $g(\eta)$, $\psi(x, \eta)$, and $\theta(x, \eta)$:

$$f''' + ff'' = 0 \quad (45)$$

$$\frac{1}{\sigma} g''' + fg'' = -Ef''^2 \quad (46)$$

$$\psi_{\eta\eta\eta} + f\psi_{\eta\eta} + \psi f'' = 2x(f'\psi_{x\eta} - \psi_x f'') + 4xg' p_{2x} - 2\sqrt{(x)}(g' f'' + gf'') \quad (47)$$

$$\frac{1}{\sigma}\theta_{\eta\eta\eta} + f\theta_{\eta\eta} = 2x(f'\theta_{x\eta} - \psi_x g'') - \psi g'' - \frac{2\sqrt{x}}{\sigma}(g'g'' + gg''') - 2E[f''\psi_{\eta\eta} + (\sqrt{x})gf''^2 + 2xp_{2x}g'f']. \quad (48)$$

Only the first of these four differential equations is nonlinear; the others are linear. Therefore $\psi(x, \eta)$ and $g(\eta)$ are linear functions of the Eckert number E, while $\theta(x, \eta)$ is a quadratic function of E.

The form of η makes $f(\eta)$ independent of the other unknowns. Equation (45) represents the classical flat plate boundary-layer problem whose solutions are well known. Once $f(\eta)$ is known, the remaining differential equations can be solved successively. However, the following boundary conditions at the wall must be satisfied:

$$\begin{aligned} \eta = 0: \quad & f = C_M, \quad f' = 0 \\ & g = 0, \quad g' = 2\frac{T_w}{T_\infty} \\ & \psi = 0, \quad \psi_\eta = 0, \quad \psi_x = 0 \\ & \theta = 0, \quad \theta_\eta = 0. \end{aligned} \quad (49)$$

The conditions $\theta(0) = 0$ follows from substituting equation (42) into equation (37) and requiring $\eta = 0$ when $y = 0$.

In order to obtain the boundary conditions for the inner solution when $\eta \to \infty$, the two solutions have to be matched. The outer expansion is first written in the inner variables $x, \bar{y}$ where $\bar{y} = y/\varepsilon$. The expansion is evaluated near the wall:

$$\begin{aligned} u &= 1 + \varepsilon U_2(x, \varepsilon\bar{y}) = 1 + \varepsilon U_2(x, 0) + 0(\varepsilon^2) \\ v &= \varepsilon V_2(x, \varepsilon\bar{y}) = \varepsilon V_2(x, 0) + 0(\varepsilon^2) \\ p &= \varepsilon P_2(x, \varepsilon\bar{y}) = \varepsilon P_2(x, 0) + 0(\varepsilon^2) \\ \rho &= 1 + \varepsilon R_2(x, \varepsilon\bar{y}) = 1 + \varepsilon R_2(x, 0) + 0(\varepsilon^2) \\ T &= 1 + \varepsilon T_2(x, \varepsilon\bar{y}) = 1 + \varepsilon T_2(x, 0) + 0(\varepsilon^2). \end{aligned} \quad (50)$$

In this particular example, all asymptotic expansions to $0(\varepsilon)$ are independent of $\bar{y}$. Since $\bar{y}$ is of the same order as η [see equation (37)], equation (50) can be considered as the asymtotic expansion of the outer solution in inner variables. Therefore, the following matching relations are obtained if only terms to $0(\varepsilon)$ are considered.

$$\begin{aligned} 1 + \varepsilon U_2(x, 0) &= \lim_{\eta\to\infty}\left(\frac{1}{2}f' + \varepsilon\frac{\sqrt{C}}{2}\psi_\eta\right) \\ V_2(x, 0) &= -\frac{1}{4}\sqrt{\left(\frac{C}{x}\right)}\lim_{\eta\to\infty}(fg' - gf') \\ P_2(x, 0) &= (\sqrt{C})p_2(x) \\ 1 + \varepsilon R(x, 0) &= \lim_{\eta\to\infty}\left[\frac{1}{2}g' + \varepsilon\frac{\sqrt{C}}{2}(\theta_\eta - \gamma M^2 p_2 g')\right]^{-1} \\ 1 + \varepsilon T_2(x, 0) &= \lim_{\eta\to\infty}\left(\frac{1}{2}g' + \varepsilon\frac{\sqrt{C}}{2}\theta_\eta\right). \end{aligned} \quad (51)$$

From these expressions, one obtains immediately the boundary conditions

$$\lim_{\eta\to\infty} f' = 2$$

$$\lim_{\eta\to\infty} g' = 2$$

$$\lim_{\eta\to\infty}(f - g) = -2\sqrt{\left(\frac{x}{C}\right)}V_2(x, 0)$$

$$\lim_{\eta\to\infty}\psi_\eta = \frac{2}{\sqrt{C}}U_2(x,0) \tag{52}$$

$$p_2(x) = \frac{1}{\sqrt{C}}P_2(x,0)$$

$$\lim_{\eta\to\infty}\theta_\eta = \frac{2}{\sqrt{C}}T_2(x,0).$$

The purpose of obtaining the inner solution is to determine the important flow properties at the wall. These are the pressure, shear stress, and heat transfer at the wall as defined in equations (14)–(16). The inner solution enables one to write directly:

$$c_{pw}(x) = \frac{p_w(x) - p_\infty}{\rho_\infty U_\infty^2} = \varepsilon P_2(x,0) = \varepsilon(\sqrt{C})p_2(x) \tag{53}$$

$$\frac{\rho_w(x)}{\rho_\infty} = \frac{T_\infty}{T_w}\left[1 + \gamma\frac{M^2}{\sqrt{C}}P_2(x,0)\right] \tag{54}$$

$$c_f(x) = \frac{\tau_w(x)}{\rho_\infty U_\infty^2} = \varepsilon\frac{1}{4}\sqrt{\left(\frac{C}{x}\right)} \times [f'' + \varepsilon(\sqrt{C})\psi_{\eta\eta}]_{\eta=0} \tag{55}$$

$$St(x) = \frac{q_w(x)}{c_p\rho_\infty U_\infty T_\infty} = -\frac{1}{4\delta}\sqrt{\left(\frac{C}{x}\right)} \times (g'' + \varepsilon(\sqrt{C})\theta_{\eta\eta})_{\eta=0}. \tag{56}$$

Only five functions are needed to evaluate the wall properties, i.e. $p_2(x)$, $f''(0)$, $\psi_{\eta\eta}(x,0)$, $g''(0)$ and $\theta_{\eta\eta}(x,0)$. These functions are in general dependent on the parameters γ, C, σ, E or M, T_w/T_∞, and C_M.

5. SOLUTION FOR THE LEADING EDGE

In this section, we carefully examine the solutions to partial differential equations, equations (47) and (48) for small values of x, i.e. in the neighborhood of the leading edge. The following expansions are assumed:

$$\psi(x,\eta) = \frac{1}{\sqrt{x}}\sum_0^N x^n F_n(\eta)$$

$$\theta(x,\eta) = \frac{1}{\sqrt{x}}\sum_0^N x^n G_n(\eta) \tag{57}$$

$$p_2(x) = \frac{1}{\sqrt{C}}P_2(x,0) = -\frac{1}{\sqrt{C}}U_2(x,0) = -\frac{1}{\sqrt{C}x}\sum_0^N B_n x^n.$$

The last equation for $p_2(x)$ is a combination of equations (27), (34) and (52). Substituting equation (57) into equations (47) and (48) and ordering the terms by powers of x, a set of ordinary differential equations results

$$F_0''' + fF_0'' + f'F_0' = \frac{2B_0}{\sqrt{C}}g' \tag{58}$$

$$F_1''' + fF_1'' - f'F_1' + 2f''F_1 = -\frac{2B_1}{\sqrt{C}}g' - 2f''g' - 2f'''g \tag{59}$$

$$\frac{1}{\sigma}G_0''' + fG_0'' + f'G_0' = -2Ef''F_0'' - 2E\frac{B_0}{\sqrt{C}}f'g' \tag{60}$$

$$\frac{1}{\sigma}G_1''' + fG_1'' - f'G_1' = -2F_1g'' - \frac{2}{\sigma}(g'g'' + gg''') - 2E[f''F_1'' + g(f'')^2 - \frac{B_1}{2\sqrt{C}}f'g'\Big]. \tag{61}$$

The boundary conditions for the system of equations (58)–(61) are

$$\eta = 0 \quad F_0 = 0 \quad F_0' = 0 \quad G_0 = 0 \quad G_0' = 0$$
$$F_1 = 0 \quad F_1' = 0 \quad G_1 = 0 \quad G_1' = 0 \tag{62}$$

$$\eta\to\infty \quad F_0' = 2\frac{B_0}{\sqrt{C}} \quad G_0' = -4E\frac{B_0}{\sqrt{C}}$$
$$F_1' = 2\frac{B_1}{\sqrt{C}} \quad G_1' = -4E\frac{B_1}{\sqrt{C}} \tag{63}$$

$$\lim_{\eta\to\infty}[f(\eta) - g(\eta)] = 2\frac{BB_0}{\sqrt{C}}. \tag{64}$$

The expressions for $F_0''(0)$ and $G_0''(0)$ can be obtained from equations (58) and (60) by a straightforward procedure. The equation for $F_0(\eta)$ may be integrated directly and the result is

$$F_0''(\eta) = F_0''(0) + \frac{2B_0}{\sqrt{C}} g(\eta) - f(\eta)F_0'(\eta). \quad (65)$$

When $\eta \to \infty$, we obtain

$$F_0''(0) = \frac{2B_0}{\sqrt{C}} \lim_{\eta\to\infty} [f(\eta) - g(\eta)] = \frac{4BB_0^2}{C}. \quad (66)$$

An analogous integration procedure for $G_0(\eta)$ from $\eta = 0$ to $\eta = \infty$ gives

$$\frac{1}{\sigma} G_0''(0) = -4E\frac{B_0}{\sqrt{C}} \lim_{\eta\to\infty} f(\eta) + 2E \times \left[\int_0^\infty f''F_0'' \, d\eta + \frac{B_0}{\sqrt{C}} \int_0^\infty f'g' \, d\eta \right] = 0. \quad (67)$$

The integrals in equation (67) have been calculated by using the expressions given in equation (65). This interesting result has also been noted by Maslen [19].

The mass-transfer parameter C_M directly influences f and, due to the nonlinearity of the equation for f, cannot be assumed to be linear in the system. If, however, the parameter C_M is taken to be small, all functions can be expressed as linear combinations. For example, we can write

$$f(\eta) = f_0(\eta) + C_M f_1(\eta) \quad (68)$$

$$g(\eta) = g_0(\eta) + C_M g_1(\eta) \quad (69)$$

which yields a set of differential equations

$$f_0''' + f_0 f_0'' = 0$$

$$f_1''' + f_0 f_1'' + f_0'' f_1 = 0$$

$$\frac{1}{Pr} g_0''' + f_0 g_0'' = -E(f_0'')^2 \quad (70)$$

$$\frac{1}{Pr} g_1''' + f_0 g_1'' = -f_1 g_0'' - 2Ef_0''f_1''$$

with the boundary conditions

$$\begin{aligned} \eta = 0: \quad & f_0 = 0 \quad f_0' = 0 \quad g_0 = 0 \quad g_0' = 2\frac{T_w}{T_\infty} \\ & f_1 = 1 \quad f_1' = 0 \quad g_1 = 0 \quad g_1' = 0 \\ \eta \to \infty \quad & f_0' = 2 \quad g_0' = 2 \\ & f_1' = 0 \quad g_1' = 0. \end{aligned} \quad (71)$$

An analogous procedure for small C_M can be carried out for the functions F_0, F_1, G_0 and G_1. Exact calculations showed that a linear approximation using C_M introduces an error of less than 1 per cent for $|C_M| < 0{\cdot}1$.

The solution to the system of equations can be used to evaluate the wall properties defined in equations (53)–(56):

$$c_{pw}(x) = -\varepsilon(B_0 x^{-\frac{1}{2}} + B_1 x^{\frac{1}{2}} + \ldots) + O(\varepsilon^2) \quad (72)$$

$$c_f(x) = \varepsilon\frac{1}{4}\sqrt{\left(\frac{C}{x}\right)}\{f''(0) + \varepsilon(\sqrt{C})\,[F_0''(0)x^{-\frac{1}{2}} + F_1''(0)x^{\frac{1}{2}} + \ldots]\} + O(\varepsilon^3) \quad (73)$$

$$St(x) = -\varepsilon\frac{1}{4\sigma}\sqrt{\left(\frac{C}{x}\right)}\{g''(0) + \varepsilon(\sqrt{C}) \times [G_1''(0)x^{\frac{1}{2}} + \ldots]\} + O(\varepsilon^3). \quad (74)$$

The coefficients in these expressions, i.e. the second derivatives of velocity and temperature at the wall, are functions of the wall temperature T_w/T_∞, the Eckert number E, and the mass-transfer parameter C_M, which, however, will be assumed to be small. The term proportional to $F_0''(0)$ gives the effect of displacement without wall curvature and is hence identical with the displacement effect on a flat plate. It can be seen that the term is proportional to ε^2/x, which is independent of the radius of curvature and identical to that found in the solution for the flat plate by Maslen [19]. According to equation (74), the heat transfer is unaffected by displacement thickness, a result which has also been noted by Maslen [19] (see also Hayes and Probstein [20]). The shear stress at the wall resulting from displacement does not disappear

at the leading edge but is proportional to x^{-1}. This leads to the result that the integral for the overall wall shear stress does not converge. This is clearly due to the singularity existing at the leading edge. Within the context of the theory of asymptotic expansions, in which the second-order solutions are linear corrections to the first-order flow, the displacement effect can be regarded only as a linear correction in the sense of weak viscous interaction. In the neighborhood of the leading edge, it is clear that a strong viscous interaction obtains. This cannot be treated here.

The influence of curvature on the flow and temperature, which is given by the terms proportional to $F_1''(0)$, and $G_1''(0)$, respectively, can be separated formally into two parts. The first part, regarded as pure curvature effect, results from additional terms appearing in the inner expansion for the flow. The second part, which we denote as interaction effects, results from the displacement effect. For the same boundary layer displacement thickness, this latter effect is weaker for the cylinder than for the flat plate. For the same reason, the surface pressure along a cone whose axis is parallel to the flow is less than that about a similarly placed wedge with the same angle.

6. NUMERICAL RESULTS

A. *Solid wall*

The system of equations (58)–(61) and (70) with the boundary conditions given by equations (62)–(64) and (71) was solved numerically for $\sigma = 0{\cdot}72$. In the case of the solid wall ($C_M = 0$) equations (72)–(74) give the following expressions for wall functions

$$c_{pw}(x) = \varepsilon\sqrt{(C)}\left(\frac{1}{B\sqrt{x}} - \frac{\sqrt{x}}{B^2}\right)\left[0{\cdot}8604 - 0{\cdot}9703\left(1 - \frac{T_w}{T_\infty}\right) + 0{\cdot}2878\,E\right] \tag{75}$$

$$c_f(x) = \varepsilon\sqrt{\left(\frac{C}{x}\right)}\left\{0{\cdot}3321 + \frac{\varepsilon}{B}\sqrt{\left(\frac{C}{x}\right)}\left[0{\cdot}8604 - 0{\cdot}9703\left(1 - \frac{T_w}{T_\infty}\right) + 0{\cdot}2878\,E\right]^2 + \frac{\varepsilon\sqrt{(Cx)}}{B^2} \times \left[1{\cdot}1656 - 0{\cdot}5700\left(1 - \frac{T_w}{T_\infty}\right) + 0{\cdot}1276\,E\right] \times \left[1 - 1{\cdot}1278\left(1 - \frac{T_w}{T_\infty}\right) + 0{\cdot}3345\,E\right] + \varepsilon\sqrt{(Cx)}\left[0{\cdot}6943 - 0{\cdot}4894\left(1 - \frac{T_w}{T_\infty}\right) + 0{\cdot}0909E\right]\right\} \tag{76}$$

$$St(x) = -\frac{\varepsilon}{\sigma}\sqrt{\left(\frac{C}{x}\right)}\left\{0{\cdot}2956\left(1 - \frac{T_w}{T_\infty}\right) + 0{\cdot}2506\,E + \varepsilon\frac{E\sqrt{(Cx)}}{B^2}\left[0{\cdot}2151 - 0{\cdot}0935 \times \left(1 - \frac{T_w}{T_\infty}\right) + 0{\cdot}2505\,E\right] \times \left[1 - 1{\cdot}1278 \times \left(1 - \frac{T_w}{T_\infty}\right) + 0{\cdot}3345\,E\right] + \varepsilon\sqrt{(Cx)} \times \left[0{\cdot}6659\left(1 - \frac{T_w}{T_\infty}\right) + 0{\cdot}5198\,E - 0{\cdot}4560 \times \left(1 - \frac{T_w}{T_\infty}\right)^2 - 0{\cdot}2798\,E\left(1 - \frac{T_w}{T_\infty}\right) + 0{\cdot}0665\,(E)^2\right]\right\}. \tag{77}$$

The pressure distribution on the wall [see equation (75)] is a second-order effect which results directly from the displacement caused by the first-order boundary layer. The expression for the pressure is a composite of two parts, each having a different dependence on x. The first part is identical with the flat plate result of Maslen [19]. This is clear by inspection because $\varepsilon/\sqrt{x}$ is independent of the radius of curvature. The second part, proportional to $\varepsilon\sqrt{x}$, gives the influence of transverse curvature on the displacement. Therefore, the second part contains both the transverse curvature as well as the displacement. It will hence be called the Interaction Effect. It reduces the pressure from that found

on the flat plate as expected. Although both terms have a different dependence on x, both give a pressure drop so that they have a similar second-order effect on the boundary layer.

The numerical values in the brackets in equation (75) agree very well with those given for $\sigma = 0{\cdot}725$ by Hayes and Probstein [20], equation (9.2.5b):

$\sigma = 0{\cdot}72$	$\sigma = 0{\cdot}725$
0·8604	0·865
0·9703	0·968
0·2878	0·289

The pressure distribution resulting from boundary-layer displacement is directly related to the problem of weak interaction (Hayes and Probstein [20]). The interaction parameter, which has been defined for high Mach number flows on flat plates, cones, and wedges, is:

$$\chi = \frac{\varepsilon(\sqrt{C})M^3}{\sqrt{x}}. \tag{78}$$

Using this parameter, equation (75) may be written:

$$\frac{p_w(x)}{P_\infty} - 1 = \gamma\left(1 - \frac{C\varepsilon^2 M^5}{\gamma^2}\right)\frac{\gamma}{M^2}\left[0{\cdot}8604 - 0{\cdot}9703\left(1 - \frac{T_w}{T_\infty}\right) + 0{\cdot}2878\,E\right]. \tag{79}$$

It has been assumed that $M \gg 1$, so that

$$B \sim M. \tag{80}$$

For the same reason, equation (79) may be written

$$\frac{p_w(x)}{p_\infty} - 1 = \gamma\left(1 - \frac{C\varepsilon^2 M^5}{\gamma}\right)\left[0{\cdot}9703\,\frac{\gamma}{M^2} \times \left(\frac{T_w}{T_\infty} - 1\right) + 0{\cdot}1439\gamma(\gamma - 1)\right]. \tag{81}$$

An important role is played by the first-order adiabatic wall temperature

$$\frac{T_{wa}}{T_\infty} = 1 + 0{\cdot}8478\,E. \tag{82}$$

Substituting the adiabatic wall temperature into equation (81) with $\gamma = 1{\cdot}4$, we obtain:

$$\frac{p_w}{p_\infty} - 1 = 0{\cdot}311\,\gamma\left(1 - \frac{C\varepsilon^2 M^5}{\gamma^2}\right). \tag{83}$$

If the second term in the bracket is neglected, equation (83) gives the expression for first-order weak interaction (Hayes and Probstein [20]) and the range of validity for weak interaction is given as $0 < \chi < 4$. Strong interaction obtains for $\chi > 4$. The effect of transverse curvature is given by the second term in the parentheses and depends on χ and the combination of parameters $C\varepsilon^2 M^5$. Since the effect of transverse curvature decreases with increasing χ, we can expect in the strong interaction region where $\chi > 4$, that the role of transverse curvature will be small. The region in which this will be correct is given by:

$$\varepsilon^2 \ll \frac{1}{CM^5}. \tag{84}$$

It will be assumed that equation (84) is satisfied in subsequent considerations. Therefore, all results are valid for $\chi < 4$. For $\chi > 4$, the strong interaction solution for the flat plate can be used.

The relationship between our solution and that for the flat plate with weak interaction was illustrated only for the purpose of estimating a region of validity for our solution. In general, the weak interaction theory is concerned with two perturbation parameters: ε and $1/M$. Both parameters approach zero in such a way that the combination of these parameters $\bar{\chi} \equiv \varepsilon(M)^3$ is of order unity. In the hypersonic-flow solution, a weak shock ensues which must be coupled to the linearized potential flow solution by an intermediate inviscid layer (see Bush and Cross [21]). In the case where $M \to \infty$, great care in matching the boundary layer to the free stream is necessary as indicated in detail by Bush and Cross [21] and Stewartson [22].

– In order to estimate the errors resulting from the truncation of the series in $\sqrt{x}$ in equation (75), we consider the first neglected term. If we

include this term, then the expression in the brackets in equation (75) would be

$$\frac{1}{B\sqrt{x}} - \frac{\sqrt{x}}{B^2}\left(1 - \frac{x}{2B}\right). \tag{85}$$

If we assume an error of 10 per cent in the last term to be included, then we obtain an expression for the range of x for which the series expansion is valid:

$$x < 0{\cdot}2\,B. \tag{86}$$

Considering only high Mach numbers and assuming that no transverse curvature effects occur in the strong interaction region, the range of validity for our solutions is given by:

$$0{\cdot}1\,C\varepsilon^2 M^6 < x < 0{\cdot}2\,M. \tag{87}$$

It is difficult to estimate how far downstream the second-order solution is valid without having done the third-order theory. Estimation of the third-order contribution from transverse curvature gives a value of x above which third-order effects must be taken into account

$$x = \frac{0{\cdot}01}{C\varepsilon^2}. \tag{88}$$

It would be reasonable to expect, however, that displacement would reduce the values of x given in equation (88) for which third-order effects become important.

The induced wall pressure distribution $C_{pw}(x)$ is shown in Fig. 2 as a function of Mach number and temperature ratio, T_w/T_∞. The pressure function is positive in general and increases linearly with temperature. The dependence on Mach number is quadratic. It is interesting to note that the pressure can even be negative in a small region near $M = 1$. For all Mach numbers $M \leqslant 1{\cdot}381$, there is a temperature ratio, T_w/T_∞, for which the induced pressure distribution disappears

$$\frac{T_w}{T_\infty} = 0{\cdot}1133 - 0{\cdot}0593\,M^2. \tag{89}$$

We are concerned in this instance with very low wall temperatures. Consequently, the density near the wall is very much greater than in the free stream. Because of this high density at the wall and in the boundary layer, the mass flow in the boundary layer remains constant in spite of the velocity reduction near the wall. In some cases, the mass flow can even be greater than that in the free stream. Therefore, in the region near a Mach number of unity, the boundary layer could exert a negative displacement effect, i.e. a suction effect on the free stream.

Equations (76) and (77) can be formally written as follows:

$$\frac{c_f}{c_{f10}} = 1 + \varepsilon(\sqrt{C})\left(C_\tau(\sqrt{x}) + D_\tau\frac{1}{\sqrt{x}} + I_\tau\sqrt{x}\right) \tag{90}$$

$$\frac{St}{St_{10}} = \frac{St_1}{St_{10}} + \varepsilon(\sqrt{C})\,(C_q(\sqrt{x}) + I_q\sqrt{x}). \tag{91}$$

The indexes 1 and 10 in the subscripts indicate first-order solutions and first-order solutions

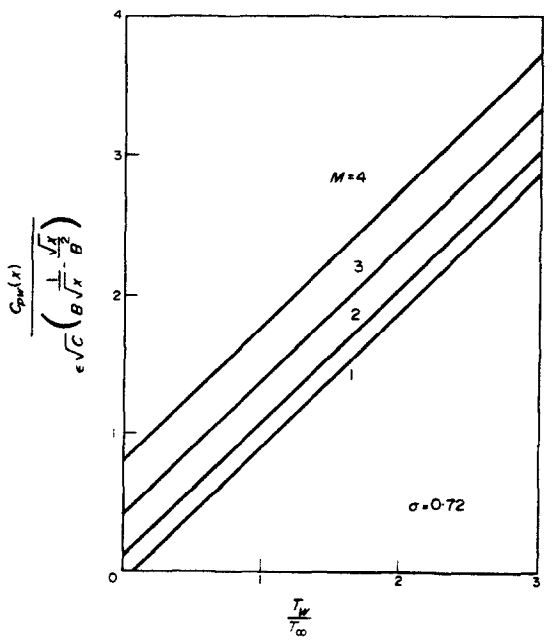

FIG. 2. Induced wall pressure distribution.

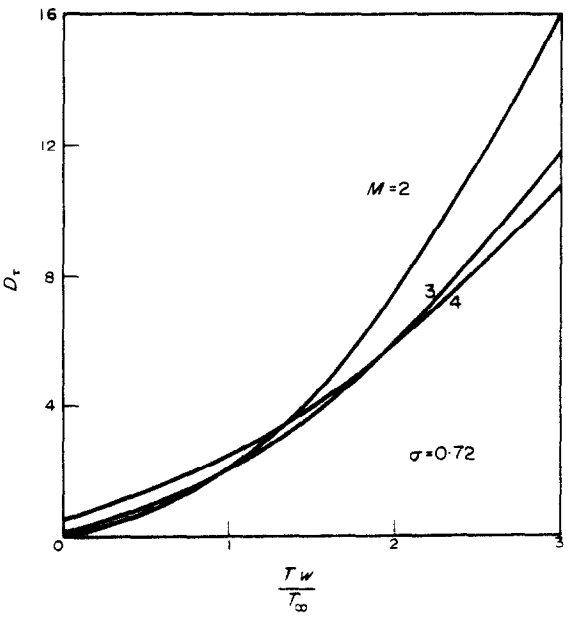

FIG. 3. Displacement effect coefficient for shear stress D_τ according to equation (90).

with $M = T_w = 0$, respectively. The functions in the parentheses represent the second-order solutions. C_τ and C_q are the transverse curvature

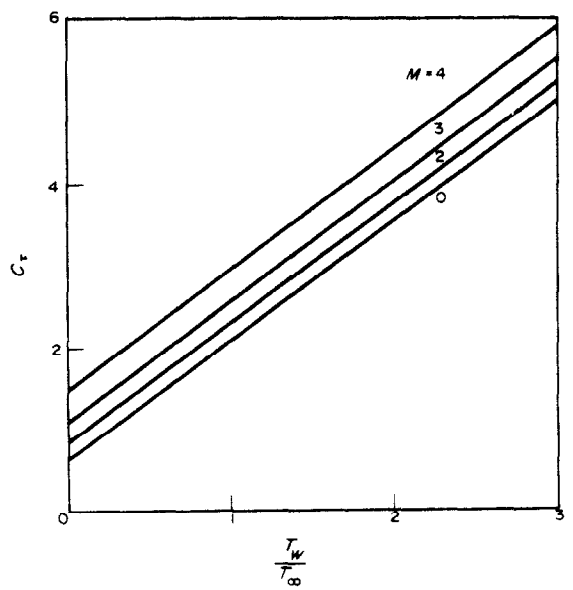

FIG. 4. Transverse curvature coefficient for shear stress C_τ according to equation (90).

effects; D_τ is the effect of displacement which occurs only for the shear stress, and I_τ and I_q are the interacting effects of transverse curvature and displacement. These functions are dependent on the Mach number and wall temperature ratio, T_w/T_∞.

The displacement coefficient, D_τ, which is identical to that for the flat plate, is shown in Fig. 3. D_τ is always positive, even in regions in which the induced wall pressure is negative.

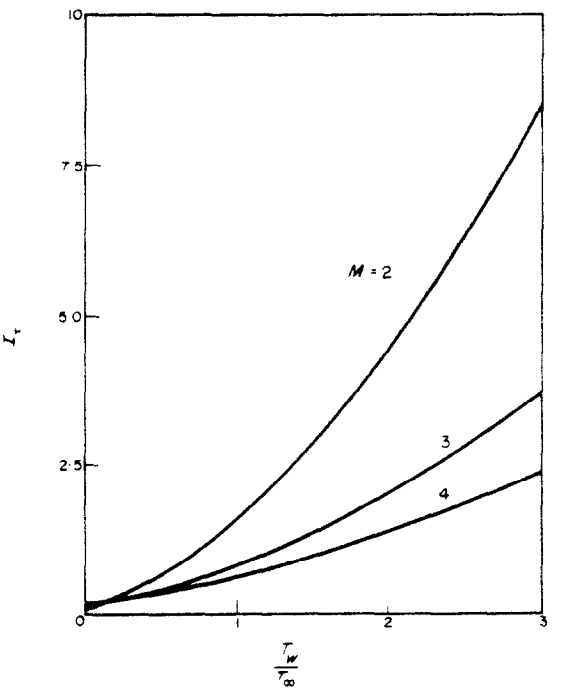

FIG. 5. Second-order interaction parameter for shear stress I_τ according to equation (90).

For values of wall temperature ratio, T_w/T_∞, given in equation (89), $D_\tau \equiv 0$. For values of the adiabatic wall temperature and high Mach number, D_τ is given by

$$D_\tau = 0{\cdot}1485\,M^3 \qquad (\gamma = 1{\cdot}4). \tag{92}$$

Neglecting curvature effects and using the definition of γ, equation (90) gives the well

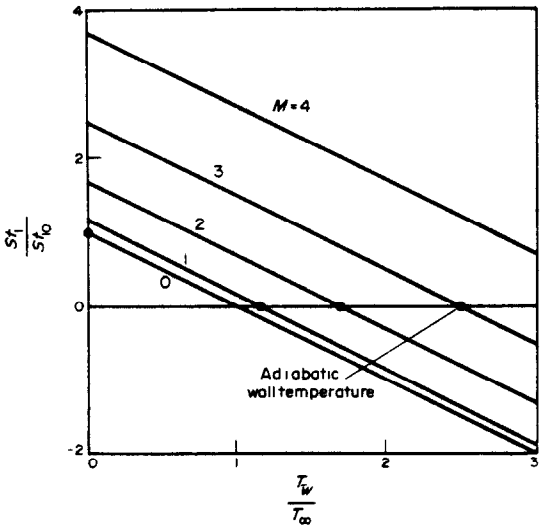

FIG. 6. First-order Stanton number.

known flat-plate weak interaction expression (Hayes and Probstein [20], equation (9.2. 26))

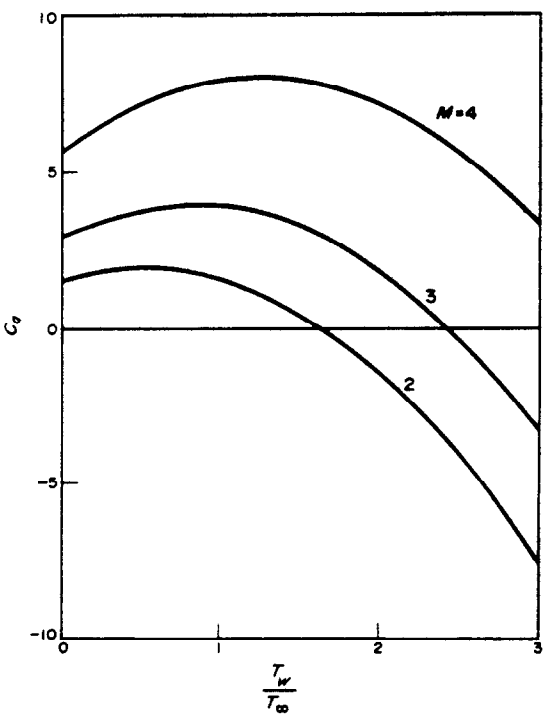

FIG. 7. Transverse curvature coefficient for heat transfer C_q according to equation (91).

$$\frac{c_f}{c_{f1}} = 1 + 0{\cdot}1485\,\gamma. \tag{93}$$

The coefficient C_τ is given in Fig. 4 as a function of M and T_w/T_∞. It is always positive and linear with the wall temperature ratio T_w/T_∞. It is a quadratic function of M. Figure 5 shows the interaction coefficient I_τ. It is also always

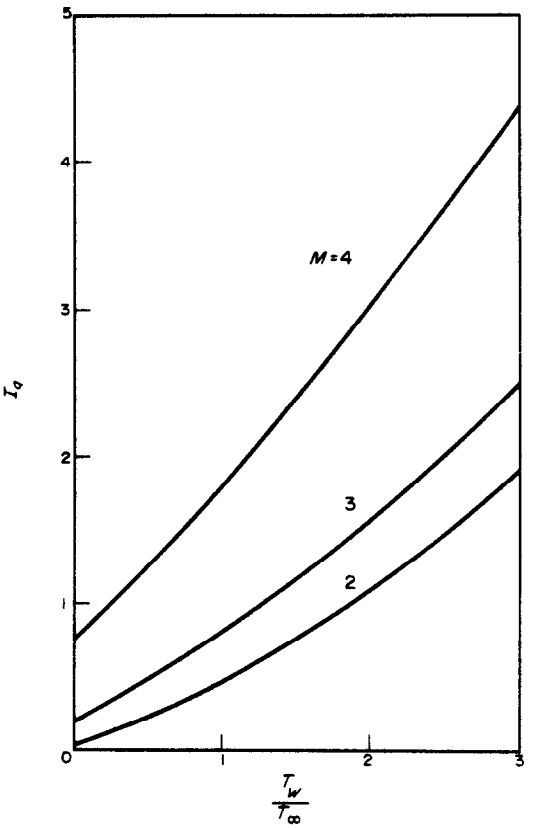

FIG. 8. Second-order interaction parameter for heat transfer I_q according to equation (91).

positive and nonlinearly dependent on T_w/T_∞. All three coefficients, D_τ, C_τ and I_τ are of the same order of magnitude.

The coefficients which occur in equation (91) are shown in Figs. 6–8. Figure 6 shows the well known behaviour of the Stanton number for the first-order boundary layer. The characteristic

zero values for the adiabatic wall temperature given by equation (82) are shown. The curves C_q as functions of wall temperature ratio in Fig. 7 show a similar behavior. For small values of the wall temperature ratio, T_w/T_∞, the curvature effect is initially positive but changes sign with increasing temperature. For each Mach number, a wall temperature ratio exists for which the curvature effect is a maximum.

It has already been indicated that there is no displacement effect on heat transfer. The interference effect is shown in Fig. 8. It is always positive and increases nonlinearly with Mach number and wall temperature ratio. For each Mach number, there is a particular temperature ratio, T_w/T_∞, for which the sum $C_q + I_q$ disappears. This means that the second-order effects considered here have no effect on the heat transfer. It should be remembered, however, that the solution given here represents an expansion in small x. The terms with higher powers of x will probably not disappear. Therefore, we conclude that the heat transfer cannot be zero for all values of x simultaneously and hence no adiabatic wall temperature can be defined for a boundary layer of higher order.

B. *Porous wall*

The porous wall treats a $1/\sqrt{x}$ wall mass flow which leads to similar solutions for the case of the flat plate. As a result of the second-order effects, however, similarity no longer obtains, equations (76) and (77) give, for this case, the following:

$$\frac{\partial c_{pw}}{\partial C_M} = -\varepsilon(\sqrt{C})\left(\frac{1}{B\sqrt{x}} - \frac{\sqrt{x}}{B^2}\right)\left[1{\cdot}027 - 0{\cdot}940\left(1 - \frac{T_w}{T_\infty}\right) + 0{\cdot}164\,E\right] \tag{94}$$

$$\frac{\partial c_f}{\partial C_M} = \varepsilon\sqrt{\left(\frac{C}{x}\right)}\left\{0{\cdot}362 - \frac{\varepsilon}{B}\sqrt{\left(\frac{C}{x}\right)} \times \left[0{\cdot}860 - 0{\cdot}970\left(1 - \frac{T_w}{T_\infty}\right) + 0{\cdot}288\,E\right] + \frac{\varepsilon\sqrt{(Cx)}}{B^2}\left\{\left[0{\cdot}102 + 0{\cdot}449\left(1 - \frac{T_w}{T_\infty}\right) - 0{\cdot}010\,E\right] \times \left[0{\cdot}860 - 0{\cdot}970\left(1 - \frac{T_w}{T_\infty}\right) - 0{\cdot}288\,E\right] - \left[1{\cdot}354 - 0{\cdot}663\left(1 - \frac{T_w}{T_\infty}\right) + 0{\cdot}148\,E\right] \times \left[1{\cdot}029 - 0{\cdot}940\left(1 - \frac{T_w}{T_\infty}\right) + 0{\cdot}107\,E\right]\right\} - \varepsilon\sqrt{(Cx)}\left[0{\cdot}197 - 0{\cdot}189\left(1 - \frac{T_w}{T_\infty}\right) + 0{\cdot}015\,E\right]\right\} \tag{95}$$

$$\frac{\partial St}{\partial C_M} = -\frac{\varepsilon}{\sigma}\sqrt{\left(\frac{C}{x}\right)}\left\{0{\cdot}270\left(1 - \frac{T_w}{T_\infty}\right) + 0{\cdot}253\,E - \varepsilon\frac{E\sqrt{(Cx)}}{B^2}\left\{\left[0{\cdot}117 - 0{\cdot}090\left(1 - \frac{T_w}{T_\infty}\right) + 0{\cdot}055\,E\right] \times \left[0{\cdot}860 - 0{\cdot}970\left(1 - \frac{T_w}{T_\infty}\right) + 0{\cdot}288\,E\right] + \left[0{\cdot}250 - 0{\cdot}109\left(1 - \frac{T_w}{T_\infty}\right) + 0{\cdot}219\,E\right] \times \left[1{\cdot}029 - 0{\cdot}940\left(1 - \frac{T_w}{T_\infty}\right) + 0{\cdot}107\,E\right]\right\} - \varepsilon\sqrt{(Cx)}\left[0{\cdot}180\left(1 - \frac{T_w}{T_\infty}\right) + 0{\cdot}160\,E - 0{\cdot}180\left(1 - \frac{T_w}{T_\infty}\right)^2 - 0{\cdot}134\,E\left(1 - \frac{T_w}{T_\infty}\right) + 0{\cdot}012\,E^2\right]\right\}. \tag{96}$$

If we normalize the skin friction to the first-order value and the Stanton number at $M = 0$ and $T_w = 0$ (both cases for the solid wall), then we may write equations (95) and (96) as:

$$\frac{\partial}{\partial C_M}\left(\frac{c_f}{c_{f10}}\right) = \frac{\partial}{\partial C_M}\left(\frac{c_{f1}}{c_{f10}}\right) + \varepsilon\sqrt{(Cx)}\left(\frac{\partial C_\tau}{\partial C_M} + \frac{\partial C_\tau}{\partial C_M}\frac{1}{x} + \frac{\partial I_\tau}{\partial C_M}\right) \quad (97)$$

$$\frac{\partial}{\partial C_M}\left(\frac{St}{St_{10}}\right) = \frac{\partial}{\partial C_M}\left(\frac{St_1}{St_{10}}\right) + \varepsilon\sqrt{(Cx)}\left(\frac{\partial C_q}{\partial C_M} + \frac{\partial I_q}{\partial C_M}\right). \quad (98)$$

Equations (97) and (98) give the effect of mass transfer at the wall on the second-order effects. Figures 9–11 show the three terms in equation (98), $(\partial/\partial C_M)(St_1/St_{10})$, $\partial C_q/\partial C_M$, and $\partial I_q/\partial C_M$ as functions of the Mach number, M, and wall temperature ratio, T_w/T_∞. Figure 9 shows the effect of mass injection at the wall on the first-order Stanton-number. The behavior of the function $(\partial/\partial C_M)(St_1/St_{10})$ is very similar to that of the Stanton number itself shown in Fig. 6. First, it is noted that for every value of the Mach number there is a wall temperature T_w/T_∞, for which $(\partial/\partial C_M)(St_1/St_{10}) = 0$; i.e. injection or suction has absolutely no effect on the Stanton number. As the Mach number increases, the effect of mass transfer increases. This implies that a given *increase* in suction effects a greater

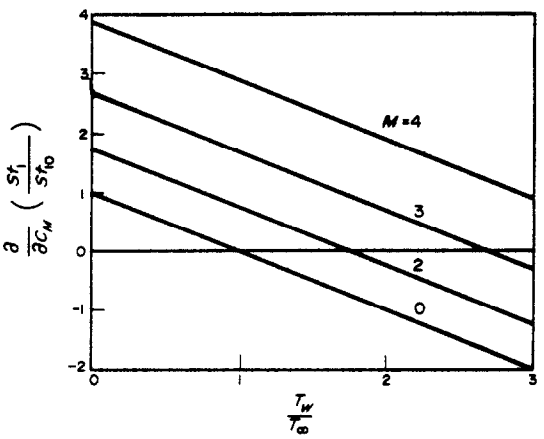

FIG. 9. The effect of wall mass transfer ($1/\sqrt{x}$ distribution) on the first-order Stanton number. Index 0 refers to $M = 0$, $T_w = 0$.

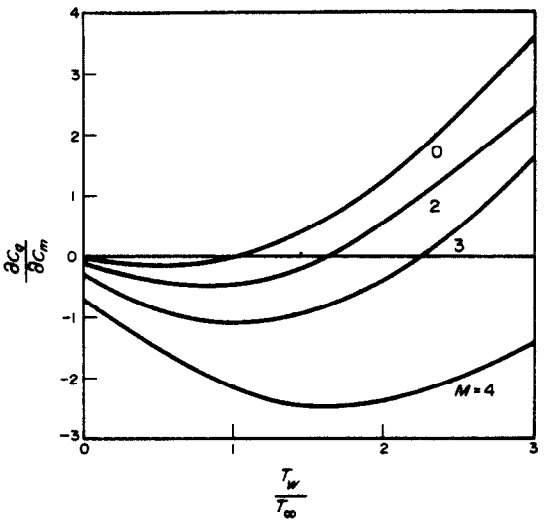

FIG. 10. The effect of wall mass transfer ($1/\sqrt{x}$ distribution) on the transverse curvature coefficient for heat transfer (see equation (98)).

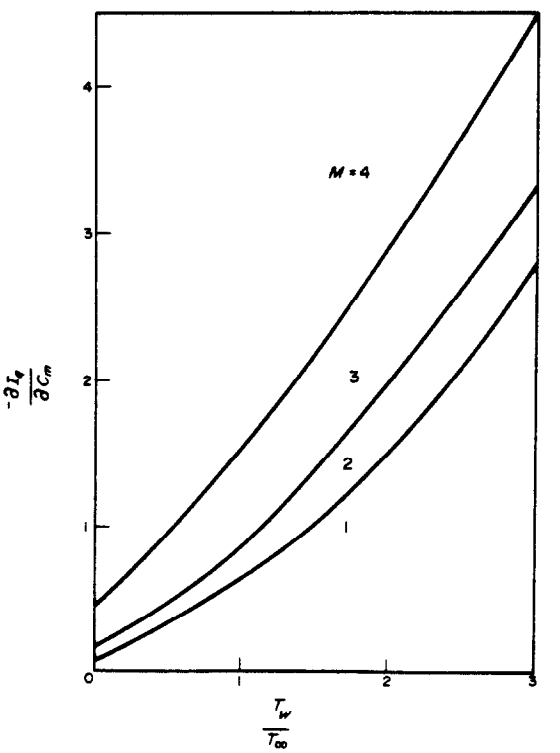

FIG. 11. The effect of wall mass transfer ($1/\sqrt{x}$ distribution) on the second-order interaction parameter for heat transfer (see equation (98)).

increase in Stanton number for higher Mach number. The Stanton number itself increases with Mach number (constant wall temperature) because the heat of dissipation deposited in the boundary layer increases the temperature gradient at the wall. Suction reduces the boundary-layer thickness and hence increases the gradient; the magnitude of this change increases with Mach number. At a constant Mach number, increasing the wall temperature reduces the effect of suction and ultimately the sign of derivative will change. For values of the wall temperature below the adiabatic temperature, increasing the wall temperature increases the thickness of the boundary layer and reduces the temperature gradient. This also reduces the effect of wall suction on the temperature gradient and, hence, the Stanton number. As indicated above, a wall temperature is reached (at a particular Mach number) at which no effect of mass transfer on Stanton number is observed. As the wall temperature is increased further, the sign of the derivative becomes negative. Increasing suction at the wall still increases the flow of heat but the negative temperature gradient at the wall changes the sign of the derivative.

Figure 10 shows the effect of wall mass transfer on the second-order curvature effect. There is, as in the case of the Stanton number, a wall temperature (for a particular Mach number) at which suction or injection at the wall have no effect on the curvature parameter. For values of the wall temperature below this value, the effect of suction is to reduce the curvature effect. This results directly from the concomitant reduction in boundary-layer thickness. As the wall temperature is increased, this effect is reversed: i.e. increased suction *increases* the curvature effect. This reversal is due to the fact that at higher temperatures the increased heat transfer resulting from the wall suction has a greater effect on increasing the boundary-layer thickness than the mass depletion from the suction itself. The net result is an increase in boundary-layer thickness and hence in the curvature effect.

The interaction effect is always negative, i.e. increasing the suction always decreases the interaction between the curvature and displacement effects. Injection at the wall always results in the reverse effect. At higher temperatures and Mach numbers, when the boundary layer is thicker, the interaction effect is always greater.

REFERENCES

1. M. VAN DYKE, Higher approximations in boundary layer theory, Part 1. General analysis, *J. Fluid Mech.* **14**, 161–177 (1962).
2. M. Van DYKE, *Perturbation Methods in Fluid Mechanics*. Academic, New York (1964).
3. M. VAN DYKE, Higher order boundary layer theory, *Ann. Rev. Fluid Mech.* **1**, 265–292 (1969).
4. M. VAN DYKE, A survey of higher order boundary layer theory in nonreacting and chemically reacting viscous flows over a hyperboloid at hypersonic condition, edited by C. H. LEWIS, AGARDograph No. 147, pp. 1–12 (1970).
5. M. VAN DYKE, Higher approximations to boundary layer theory, Part 3. Parabola in uniform stream, *J. Fluid Mech.* **19**, 145–160 (1964).
6. L. DEVAN, Second-order incompressible laminar boundary layer development on a two-dimensional semi-infinitive body, Ph.D. Dissertation, School of Engineering, University of California at Los Angeles (1964).
7. K. GERSTEN and J. F. GROSS, Mass-transfer effects on higher-order boundary layer solutions: The leading edge of a swept cylinder, *Int. J. Heat Mass Transfer* **16**, 65–79 (1973).
8. K. GERSTEN, J. F. GROSS and G. G. BÖRGER. Die Grenzschicht höherer Ordnung an der Staulinie eines schiebenden Zylinders mit starkem Absaugen oder Ausblasen, *Z. Flugwiss.* **20** (9), 330–341 (1972).
9. R. A. SEBAN and R. BOND, Skin-friction and heat-transfer, characteristics of a laminar boundary layer on a cylinder in axial incompressible flow, *J. Aeronaut. Sci.* **18**, 671–675 (1951).
10. H. R. KELLY, A note on the laminar boundary layer on a circular cylinder in axial incompressible flow, *J. Aeronaut. Sci.* **21**, 634 (1954).
11. J. C. COOKE, The flow of fluids along cylinders, *Q. J. Mech. Appl. Math.* **10**, 312 (1951).
12. M. B. GLAUERT and M. T. LIGHTHILL, The axisymmetric boundary layer on a long thin cylinder, *Proc. R. Soc., Lond.* **230A**, 188 (1955).
13. S. ESHGY and R. W. HORNBECK, Flow and heat transfer in the axisymmetric boundary layer over a circular cylinder, *Int. J. Heat Mass Transfer* **10**, 1757 (1967).
14. D. J. WANOUS and E. M. SPARROW, Longitudinal flow over a circular cylinder with surface mass transfer, *AIAA Jl* **3**, 147–149 (1965).
15. N. H. JAFFE and T. T. OKAMURA, The transverse curva-

ture effect on the incompressible laminar boundary layer for longitudinal flow over a cylinder, *ZAMP* **19**, 564–574 (1968).
16. T. CEBECI, E. R. WAGULIS and R. D. PARTIN, Effect of transverse curvature on skin friction and heat transfer in laminar flows past slender circular cylinders, *J. Heat Transfer* **90**, 485–487 (1968).
17. G. N. WARD, *Linearized Theory of Steady High-Speed Flow*. Cambridge University Press (1955).
18. C. F. DEWEY and J. F. GROSS, Exact similar solutions of the laminar boundary-layer equations, *Adv. Heat Transfer* **4**, 317–446 (1967).
19. S. M. MASLEN, Second approximation to laminar compressible boundary layer on a flat plate in slip flow, TN 2818, National Advisory Committee for Aeronautics, Washington, D.C. (1952).
20. W. D. HAYES and R. F. PROBSTEIN, *Hypersonic Flow Theory*. Academic Press, New York, (1959).
21. W. B. BUSH and A. K. CROSS, Hypersonic weak-interaction similarity solutions for flow past a flat plate, *J. Fluid Mech.* **19**, 349–359 (1967).
22. K. STEWARTSON, *The Theory of Laminar Boundary Layers in Compressible Fluids*. The Clarendon Press, Oxford (1964).

LA COUCHE LIMITE DE SECOND ORDRE LE LONG D'UN CYLINDRE CIRCULAIRE DANS UN ECOULEMENT SUPERSONIQUE

Résumé—On étudie la couche limite laminaire de second ordre le long d'un cylindre circulaire dans un écoulement supersonique avec ou sans transfert de masse en utilisant la méthode des développements asymptotiques. L'analyse donne le second ordre pour la pression, la contrainte tangentielle et le transfert thermique à la paroi. On présente des résultats numériques pour l'écoulement près du bord d'attaque.

Il y trois effets du second ordre dus à la courbure transverse. au déplacement et à l'interaction de la courbure et du déplacement.

Pour la paroi solide, les trois effets du second ordre augmentent le cisaillement et cela d'autant plus que la température de paroi augmente. Dans le cas du transfert thermique, l'effet du déplacement disparaît, l'effet d'interaction est toujours positif (accroissement du transfert thermique) et l'effet de courbure transverse est positif pour des faibles températures de paroi et négatif pour des températures élevées.

L'effet du flux massique à la paroi est généralement dans le sens prévu, c'est à dire que l'injection épaissit la couche limite et augmente les effets du second ordre tandis que l'aspiration réduit l'importance du déplacement et de la courbure transverse.

Une exception à la règle générale énoncée ci-dessus se rencontre aux températures pariétales élevées.

GRENZSCHICHT ZWEITER ORDNUNG AN EINEM KREISZYLINDER IN ÜBERSCHALLSTRÖMUNG

Zusammenfassung—Die laminare Grenzschicht zweiter Ordnung entlang eines kreisförmigen Zylinders in einer Uberschall-Strömung mit und ohne Oberflächen-Stoff-Ubertragung wird untersucht, wobei man die Methode entsprechender asymptotischer Expansionen anwendet. Insbesondere ergibt die Analyse die Terme 2. Ordnung für den Druck, die Schubbelastung, und die Wärmeübertragung an die Wand infolge der Quer-Oberflächen Erneuerung und der Verschiebung. Für die Strömung nahe der Anströmkante des Zylinders werden numerische Ergebnisse angegeben. Es gibt drei Effekte zweiten Grades; nämlich infolge der Quer-Krümmung, infolge der Verschiebung und infolge der Wechselwirkung von Krümmung und Verschiebung. Für die massive Wand vergrössern alle drei Effekte 2. Grades die Schubbelastung und dieses Ergebnis wächst mit steigender Wand-Temperatur. Im Fall der Wärmeübertragung verschwindet der Verschiebungseffekt, der Effekt der Wechselwirkung ist immer positiv (Anwachsen der Wärmeübertragung), und der Quer-Krümmungs-Effekt ist positiv für niedrige Wandtemperaturen und negativ für hohe Wandtemperaturen.

Der Effekt des Stoffstromes an der Wand liegt im allgemeinen in der erwarteten Richtung, d.h. Stoffzugabe verdichtet die Grenzschicht und vergrössert Effekte 2. Ordnung wogegen der Wandsog die Bedeutung von Verschiebung und Querkrümmung vermindert, wenn man Masse aus der Grenzschicht abzieht. Eine Ausnahme zur oben dargestellten Regel kommt bei hohen Wandtemperaturen vor.

ПОГРАНИЧНЫЙ СЛОЙ ВТОРОГО ПОРЯДКА КРУГОВОГО ЦИЛИНДРА В СВЕРХЗВУКОВОМ ПОТОКЕ

Аннотация—С помощью метода асимптотических разложений исследуется ламинарный пограничный слой второго порядка кругового цилиндра в сверхзвуковом потоке при наличии и отсутствии поверхностного массообмена. В результате анализа получены члены второго порядка для давления, касаткльного напряжения и теплообмена на стенке, вызванных поперечной кривизной поверхности и вытеснением. Представлены численные результаты для теяения у передней точки цилиндра.

Существуют три эффекта второго рода, а именно: эффекты, вызванные поперечной кривизной, вытеснением и взаимодействием кривизны и вытеснения.

В случае твердой стенки все три эффекта второго порядка увеличивают сдвиговое напряжение, и это влияние усиливается с ростом температуры стенки. В случае теплообмена эффект вытеснения отсутствует, эффект взаимодействия всегда положителен (интенсифицирует теплообмен), а эффект поперечной кривизны может быть как положительным (при низких температурах), так и отрицательным (при высоких температурах).

Влияние потока массы обычно не вызывает сомнений, т.е. вдув массы увеличивает толщину пограничного слоя и усиливает эффекты второго рода, тогда как отсос на стенке, удаляя массу из пограничного слоя, уменьшает влияние вытеснения и поперечной кривизны. Исключение из общего правила представляет случай высокой температуры стенки.